Materials Science & Engineering A 715 (2018) 41–48

Contents lists available at ScienceDirect

Materials Science & Engineering A

journal homepage: www.elsevier.com/locate/msea

Microstructure evolution and tensile properties of conventional cast TiAl-based alloy with trace Ni addition

Jianchao Han[a,*], Jing Dong[b], Shuzhi Zhang[c], Changjiang Zhang[c], Shulong Xiao[d], Yuyong Chen[d]

[a] College of Mechanical Engineering, Taiyuan University of Technology, Taiyuan 030024, China
[b] College of Environmental Science and Engineering, Taiyuan University of Technology, Taiyuan 030024, China
[c] School of Materials Science and Engineering, Taiyuan University of Technology, Taiyuan 030024, China
[d] State Key Laboratory of Advanced Welding and Joining, Harbin Institute of Technology, Harbin 150001, China

ARTICLE INFO

Keywords:
Titanium aluminides
Microstructure
Characterization
Precipitation
Tensile property

ABSTRACT

The microstructure evolution and tensile properties of Ti-48Al-2Cr-2Nb-0.25Ni alloy fabricated by the induction skull melting (ISM) process were investigated. Results showed that the influence of trace Ni addition on the cast microstructure was slight, while the γ phase fraction increased relatively. After tensile tests at elevated temperature, nanoscale τ_3 particles precipitated within the lamellar colony in the gauge area. The τ_3 phase exhibited the specific orientation relationship with the α_2 and γ phases: $(22\bar{4}2)\tau_3//(40\bar{4}1)\alpha_2//(113)\gamma$ and $[1\bar{1}00]\tau_3//[11\bar{2}0]\alpha_2//[\bar{1}10]\gamma$. At elevated temperature, the UTS and ε_f were enhanced evidently by Ni addition than that of Ti-48Al-2Cr-2Nb alloy. Dislocations were pinned by the nanoscale τ_3 precipitates during tensile deformation at elevated temperature. The nanoscale τ_3 precipitates and increased γ phase fraction induced by Ni alloying could account for the notable tensile properties in the present work. The precipitation behavior and the main strengthening mechanism were analyzed and discussed in detail.

1. Introduction

Due to the low density, specific modules, high specific temperature strength and oxidation resistance at elevated temperature, TiAl-based alloys have been attracted considerable attention as strong candidate materials for aerospace application [1–4]. Because of the high material cost and limited formability, TiAl-based alloys tend to favor near-net-shape processes such as casting. For adjusting microstructure and mechanical properties, the alloying elements, such as Nb, Cr, Mn and Mo etc. are usually added in the TiAl-based alloys [5–8]. With the combinations of ductility, toughness and creep resistance, Ti–48Al–2Cr–2Nb emerges as the first to enter commercial jet engine service [9]. However, compared with the hot-deformed TiAl alloys, the relatively low strength and ductility of Ti–48Al–2Cr–2Nb appear to be the obstacle for its further application.

In previous studies, Ni alloying is investigated to improve the mechanical properties and hot workability in TiAl-based alloys, and the results are effective [10,11]. It is also found that Ni can enlarge the γ phase zone in Ti–Al phase diagram and is beneficial to stabilize the γ phase [12]. Furthermore, the addition of Ni results in the precipitation of the Ni-riched τ_3 phase (Al_3NiTi_2) during solidification and heat treatment in the Ti-Al-Ni system, and the morphology and size differ with the relevant precipitation processes [13,14]. The τ_3 phase precipitated during solidification is coarse and detrimental to mechanical properties, while the refined τ_3 phase formed during heat treatment is proved to be beneficial for the strength [15,16]. However, the content of Ni addition in the previous researches is usually high (1 at%~), and the influence of the solid dissolved Ni element on microstructure and mechanical property is rarely reported.

The precipitation strengthening has been considered as an effective method for strength improvement at elevated temperature, with different type of precipitates, such as carbide [17–20], silicide [21,22] and nitride [23,24]. These precipitates can act as obstacles for dislocation sliding and climbing, resulting in the enhancement of strength and creep resistance [25,26]. In most researches, the secondary precipitates usually form during the corresponding solidification process or appropriate heat treatment [27–29]. In addition, the secondary precipitates can also occur during the deformation process with the assistance of the external stress and then strengthen the alloy reasonably. In Gouma's research [30], H-type carbide (Ti_2AlC) mainly precipitates in K5SC alloy aged at 900 ℃ for 48 h, while more than 3 times H-type carbides can be observed in the sample aged for 24 h and subsequently creep deformed at 760 ℃ for another 25 h. Compared with the matrix K5 alloy and K5S alloy, the strength and creep resistance at elevated temperature are enhanced evidently with the Ti_2AlC precipitates [25,31]. Furthermore, similar precipitation behavior has been reported

* Corresponding author.
E-mail address: hanjianchao@tyut.edu.cn (J. Han).

https://doi.org/10.1016/j.msea.2017.12.092
Received 24 October 2017; Received in revised form 21 December 2017; Accepted 22 December 2017
Available online 27 December 2017
0921-5093/

for P-type carbide (Ti_3AlC) [17,20] and ζ-Ti_5Si_3 [32] during the mechanical test process. This deformation induced/assisted precipitation behavior in TiAl-based alloy could be attributed to the increased rates of solid phase transformation, increased matrix or interface diffusion or the supersaturation of alloying element in local area [30,32,33]. And this could be considered as a specific and effective strengthening method for the TiAl-based alloys.

In this study, minor Ni was introduced into a conventional TiAl alloy. After a tensile test at elevated temperature, many precipitates were observed in the deformed gauge area. The aim of the present work was to reveal the microstructure evolution and tensile properties of Ni-containing Ti–48Al–2Cr–2Nb. The precipitation behavior of τ_3 phase and strengthening mechanism were discussed in detail.

2. Materials and methods

The TiAl alloy used in this work was Ti-48Al-2Cr-2Nb and Ti-48Al-2Cr-2Nb-0.25Ni (hereafter T4822 and T4822-Ni, at%). The parent materials used in this study contained Ti bar (> 99.99%), pure Al (> 99.99%), master alloy Al–Nb (52.59%), pure Cr (> 99.99%) and pure nickel powders (> 99.99%),all in wt%. An ingot weighing 600 g was prepared by the induction skull melting method under argon atmosphere (pressure of ~ 50 kPa). To improve the chemical homogeneity, thermal insulation and electromagnetic stirring were conducted for 300 s in the melt condition. The melt was poured into a 500 ℃ preheated metal mold forming a cylindrical ingot with size of Φ50 mm × 60 mm. The chemical compositions of the ingots were measured by X-ray fluorescence (AXIOS-PW4400) and listed in Table 1.

To determine the phase constituent and fraction of the specimens, X-ray diffraction (XRD) studies were performed on a X′PERT from HIT, CHINA. The measured diffractograms were evaluated with the software X′PERT Highscore based on a quantitative Rietveld analysis [34]. The microstructures were characterized by Scanning Electron Microscopy (SEM) and Transmission Electron Microscopy (TEM). SEM was conducted on a Quanta 200FEG in the back-scattered electron imaging (BSE) and secondary electron imaging (SE) mode. Transmission electron microscope (TEM) analysis was performed to determine the crystal structure on a Tecnai G2 F30 microscope operating at 300 kV. High-angle annular dark field imaging (HAADF) was conducted on a Talos F200x for elements distribution characterization. SEM-BSE observation was conducted on samples after electro-polishing. The electro-polishing was implemented at − 19 V and − 45 ℃, and the electrolyte was a solution of 6% perchloric acid + 34% butanol + 60% methanol. Thin TEM foils were prepared by mechanical polishing and twin-jet electro-polishing. The electrolyte and parameters were the same as electro-polishing.

The tensile test was performed on Instron-5500 testing machine at RT, 700 ℃, 800 ℃ and 900 ℃, driven at a crosshead speed of 0.5 mm/min. The geometry size of the tensile specimens can be seen in the previous research [4]. At least three tests were performed under each condition and average values were reported. Fracture surfaces were observed to understand fracture mechanisms.

3. Results

3.1. Microstructure characterization

Fig. 1 shows the XRD patterns of as-cast T4822 and T4822-Ni alloys.

Table 1
Measured chemical compositions (in wt%) of the studied alloys.

Alloys	Al	Cr	Nb	Ni	O	N	Ti
T4822	32.75	2.65	4.78	–	0.07	0.01	Bal.
T4822-Ni	33.31	2.71	4.73	0.39	0.08	0.01	Bal.

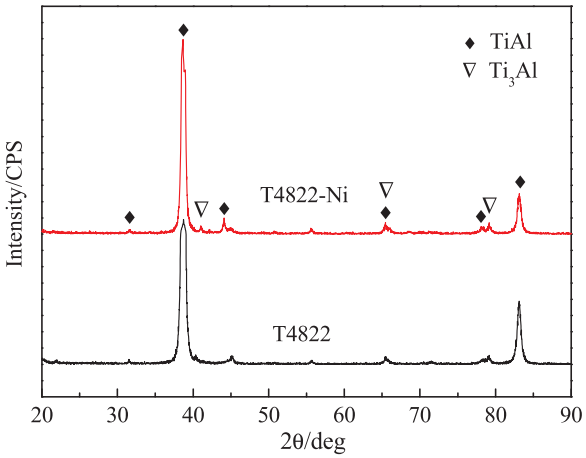

Fig. 1. XRD patterns of T4822 and T4822-Ni alloys.

Table 2
Microstructure features of as-cast T4822 and T4822-Ni alloys.

Alloy	Grain size (μm)	Lamellae width (nm)	Phase fraction (vol%)	
			γ	α_2
T4822	800 ± 100	350 ± 15	79	21
T4822-Ni	780 ± 100	365 ± 20	85	15

It is shown that the phase constitution of the two alloys is similar, consisting of dominant γ and α_2 phases. From the XRD data, the phase fractions of each phase are determined and given in Table 2. As regard the matrix alloy, the phase fractions of γ and α_2 phase were 79 and 21 (vol%), while in the Ni-containing alloy, the phase fractions of the two phases were detected as 85 and 15 (vol%), respectively. It can be obtained that with the Ni addition, the γ phase fraction is increased slightly, while the tendency of α_2 phase fraction is opposite.

Fig. 2 shows the microstructure of as-cast T4822 and T4822-Ni alloys. A nearly fully lamellar microstructure with nonlinear colony boundary is obtained in the both alloys. Small bulk γ grains can be observed and mainly distribute around the lamellar colonies, as arrowed. It is noteworthy that the number of bulk γ grains is relatively larger in Ni-containing alloy than the matrix alloy. Moreover, evident dendrite microstructure with dark and bright contrasts can be clearly observed in Fig. 2a) and b), which are called as the Al segregation and β segregation. Measured by the linear intercept method, the mean grain size of the as-cast T4822 and T4822-Ni alloys were 800 μm and 780 μm , respectively. This means that the influence of Ni addition on the grain size is slight.

Fig. 3 shows TEM images of as-cast T4822 and T4822-Ni alloys in the edge-on condition, in which α_2 and γ phase satisfy the Blackburn orientation relationship (Fig. 3c) [35]. For each material, about 250 lamellae from at least eight different lamellar colonies were examined. The mean lamellae width of T4822 and T4822-Ni were measured as 350 nm and 365 nm, respectively. The lamellae width appears to be thickened slightly by the trace Ni addition. According to the TEM observations, the lamellae is straight and clear, and there is no secondary precipitate in the lamellae interface or along the grain boundary in both alloys.

3.2. Tensile properties and fractography

Fig. 4 shows the results of the tensile tests and the scatter of the measured tensile properties as function of the test temperature of T4822. At room temperature, the ultimate tensile strength (UTS) of T4822-Ni alloy is 550 MPa, which is 4% higher than that of the matrix